Geophysical Research Letters

RESEARCH LETTER
10.1029/2019GL084379

Special Section:
Initial results of the ERG (Arase) project and multi-point observations in geospace

Remote Detection of Drift Resonance Between Energetic Electrons and Ultralow Frequency Waves: Multisatellite Coordinated Observation by Arase and Van Allen Probes

M. Teramoto[1,2], T. Hori[1], S. Saito[1], Y. Miyoshi[1], S. Kurita[1], N. Higashio[3], A. Matsuoka[4], Y. Kasahara[5], Y. Kasaba[6], T. Takashima[4], R. Nomura[7], M. Nosé[1], A. Fujimoto[8], Y.-M. Tanaka[9,10,11], M. Shoji[1], Y. Tsugawa[1], M. Shinohara[12], I. Shinohara[4], J. B. Blake[13], J.F. Fennell[13], S.G. Claudepierre[13,14], D. L. Turner[13], C. A. Kletzing[15], D. Sormakov[16], and O. Troshichev[16]

[1]Institute for Space-Earth Environmental Research, Nagoya University, Nagoya, Japan, [2]Faculty of Engineering, Kyushu Institute of Technology, Fukuoka, Japan, [3]Research and Development Directorate, Japan Aerospace Exploration Agency, Tsukuba, Japan, [4]Institute of Space and Astronautical Science, Japan Aerospace Exploration Agency, Sagamihara, Japan, [5]Graduate School of Natural Science and Technology, Kanazawa University, Kanazawa, Japan, [6]Graduate School of Science, Tohoku University, Sendai, Japan, [7]National Astronomical Observatory of Japan, Mitaka, Japan, [8]Faculty of Computer Science and Systems Engineering, Kyushu Institute of Technology, Fukuoka, Japan, [9]National Institute of Polar Research, Tachikawa, Japan, [10]Polar Environment Data Science Center, Joint Support-Center for Data Science Research, Research Organization of Information and Systems, Tachikawa, Japan, [11]Department of Polar Science, School of Multidisciplinary Sciences, The Graduate University for Advanced Studies, Tachikawa, Japan, [12]Kagoshima National College of Technology, Kirishima, Japan, [13]Space Sciences and Applications Laboratory, Aerospace Corporation, El Segundo, CA, USA, [14]Department of Atmospheric and Oceanic Sciences, University of California, Los Angeles, CA, USA, [15]Department of Physics and Astronomy, University of Iowa, Iowa City, IA, USA, [16]Department of Geophysics, Arctic and Antarctic Research Institute, St. Petersburg, Russia

Key Points:
- Arase observed flux modulations of relativistic electrons at 04 MLT without variations in the ambient magnetic and electric fields
- Time-of-flight analysis from the energy dispersion of relativistic electrons identified the drift-resonant region to be 14–18 MLT
- The interactions between Pc5 waves and relativistic electrons occurred at a limited local time even though the estimated *m* number is small

Supporting Information:
- Supporting Information S1

Correspondence to:
M. Teramoto,
teramoto.mariko418@mail.kyutech.jp

Citation:
Teramoto, M., Hori, T., Saito, S., Miyoshi, Y., Kurita, S., Higashio, N., et al. (2019). Remote detection of drift resonance between energetic electrons and ultralow frequency waves: Multisatellite coordinated observation by Arase and Van Allen Probes. *Geophysical Research Letters*, *46*, 11,642–11,651. https://doi.org/10.1029/2019GL084379

Received 2 JUL 2019
Accepted 18 SEP 2019
Published online 5 NOV 2019

Abstract We report the electron flux modulations without corresponding magnetic fluctuations from unique multipoint satellite observations of the Arase (Exploration of Energization and Radiation in Geospace) and the Van Allen Probe (Radiation Belt Storm Probe [RBSP])-B satellites. On 30 March 2017, both Arase and RBSP-B observed periodic fluctuations in the relativistic electron flux with energies ranging from 500 keV to 2 MeV when they were located near the magnetic equator in the morning and dusk local time sectors, respectively. Arase did not observe Pc5 pulsations, while they were observed by RBSP-B. The clear dispersion signature of the relativistic electron fluctuations observed by Arase indicates that the source region is limited to the postnoon to the dusk sector. This is confirmed by RBSP-B and ground-magnetometer observations, where Pc5 pulsations are observed to drift-resonate with relativistic electrons on the duskside. Thus, Arase observed the drift-resonance signatures "remotely," whereas RBSP-B observed them "locally."

Plain Language Summary Magnetohydrodynamic waves in the outer radiation belt with periods of ~150–250 s occasionally cause the acceleration of energetic electrons drifting eastward around the Earth. We examined the longitudinal distributions of the interaction region in which magnetohydrodynamic waves with periods of ~150–250 s interacted with energetic electrons on 30 March 2017, using simultaneously observed data by multisatellite observations from the Arase and the Radiation Belt Storm Probe (RBSP)-B satellites. Both satellites observed radiation belts at different local times but at almost the same Earth radii. The Arase satellite located in the dawn sector observed energetic electron flux modulations that had clear energy dispersion signatures, while magnetohydrodynamic waves with the same period were not identified. However, the RBSP-B located in the dusk sector simultaneously observed magnetohydrodynamic waves and the energetic electron modulations with the characteristics of the interaction. This multipoint measurement indicates that the interaction region is limited from the postnoon to the dusk sector.

1. Introduction

Ultralow frequency (ULF) waves, especially Pc5 pulsations with a frequency of 2–7 mHz in the inner magnetosphere, play an important role in the acceleration of energetic electrons in the outer radiation belt (e.g., Shprits et al., 2008). It is thought that the drift resonance between the ULF waves and the drifting

electrons leads to this acceleration and contributes to flux enhancements of the outer radiation belt (Elkington et al., 1999).

The drift-resonance condition is given by the following equation (Southwood et al., 1969):

$$\omega - m\omega_{\mathrm{d}} = 0 \tag{1}$$

where ω, ω_{d}, and m are the angular frequency of the wave, the angular drift frequency of the electron, and the azimuthal wave number (m number) of the wave, respectively.

Comparing the pulsation power with ground observations and the energetic electron flux in the outer radiation belt based on measurements of the geostationary satellite GOES7, Mathie and Mann (2000) determined that the MeV electron flux in a geostationary orbit increases during extended intervals of enhanced ULF pulsation power. They suggested that ULF waves cause an acceleration of relativistic electrons, generating storm-time electrons via drift resonance. The results of satellite observations have shown simultaneous modulations of the energetic electron flux and the ambient magnetic field and the drift resonance between them (Claudepierre et al., 2013; Tan et al., 2004; Zong et al., 2009).

The radial transport of trapped particles has been modeled as radial diffusion. The radial diffusion coefficients have been estimated assuming that the modulations between ULF wave and drifting electrons occur over all Magnetic Local Times (MLTs; e.g., Ozeke et al., 2013; Walt, 1994). In this case, the modulations of both the ambient electric (magnetic) fields and the electron flux should be observed simultaneously. However, observed ULF waves have local time asymmetry of the amplitude and azimuthal wave numbers (e.g., Rae et al., 2005; Tan et al., 2011). Therefore, it is expected that the energetic electron fluxes would be modulated by the ULF waves at specific local times, and these electron flux modulations will be observed at different local times. To evaluate the radial transport as well as the acceleration of energetic electrons by ULF waves, it is important to identify the longitudinal distribution of the modulation region between the ULF waves and the electrons.

In the present paper, we present observational results obtained with the Arase and Radiation Belt Storm Probe (RBSP)-B satellites on 30 March 2017, when both satellites observed radiation belts at different MLTs but the same L-shell. Using time-of-flight analysis for the energetic electron modulations observed by both satellites and the data from the ground observations, we identify the modulation region of the energetic electrons due to the ULF waves. We also show that the actual interactions occur at specific MLTs even though the estimated mode number, m, is relatively small.

2. Data

In this study, we have used energetic electron, magnetic, and electric field data obtained from the Extremely High-Energy Electron Experiment (XEP; Higashio et al., 2018), the Magnetic Field instrument (MGF; Matsuoka et al., 2018), and the Electric Field Detector (EFD; Kasaba et al., 2017; Kasahara et al., 2018), onboard the Arase satellite (Miyoshi et al., 2018). The XEP provides differential electron flux data for relativistic energies from 400 keV to 20 MeV. The spin-averaged flux data were used with a time resolution of 8 s.

We used the RBSP-B data for this study, which reached apogee at ~18 MLT when the Arase satellite was located at its apogee at ~04 MLT. The Magnetic Electron Ion Spectrometers (MagEIS; Blake et al., 2013) onboard the two RBSP spacecraft. We used the electron flux data observed by the MagEIS covering the energy range from ~460 keV to 2.6 MeV. We also used the magnetic field data observed by the Electric and Magnetic Field Instrument Suite and Integrated Science (EMFISIS) experiment (Kletzing et al., 2013). The magnetic field and spin-averaged electron flux data were used with resolutions of 4 and 11 s, respectively.

3. Observations and Analysis

Figure 1a displays the solar wind speed, solar wind number density, the Z component of the interplanetary magnetic field in the Geocentric Solar Magnetospheric coordinate system, and the SYM-H and auroral electrojet (AE) indices from 0400 to 0800 UT on 30 March 2017. This interval corresponds to the storm recovery phase beginning from 27 March. Typical Alfvénic fluctuations embedded in the high-

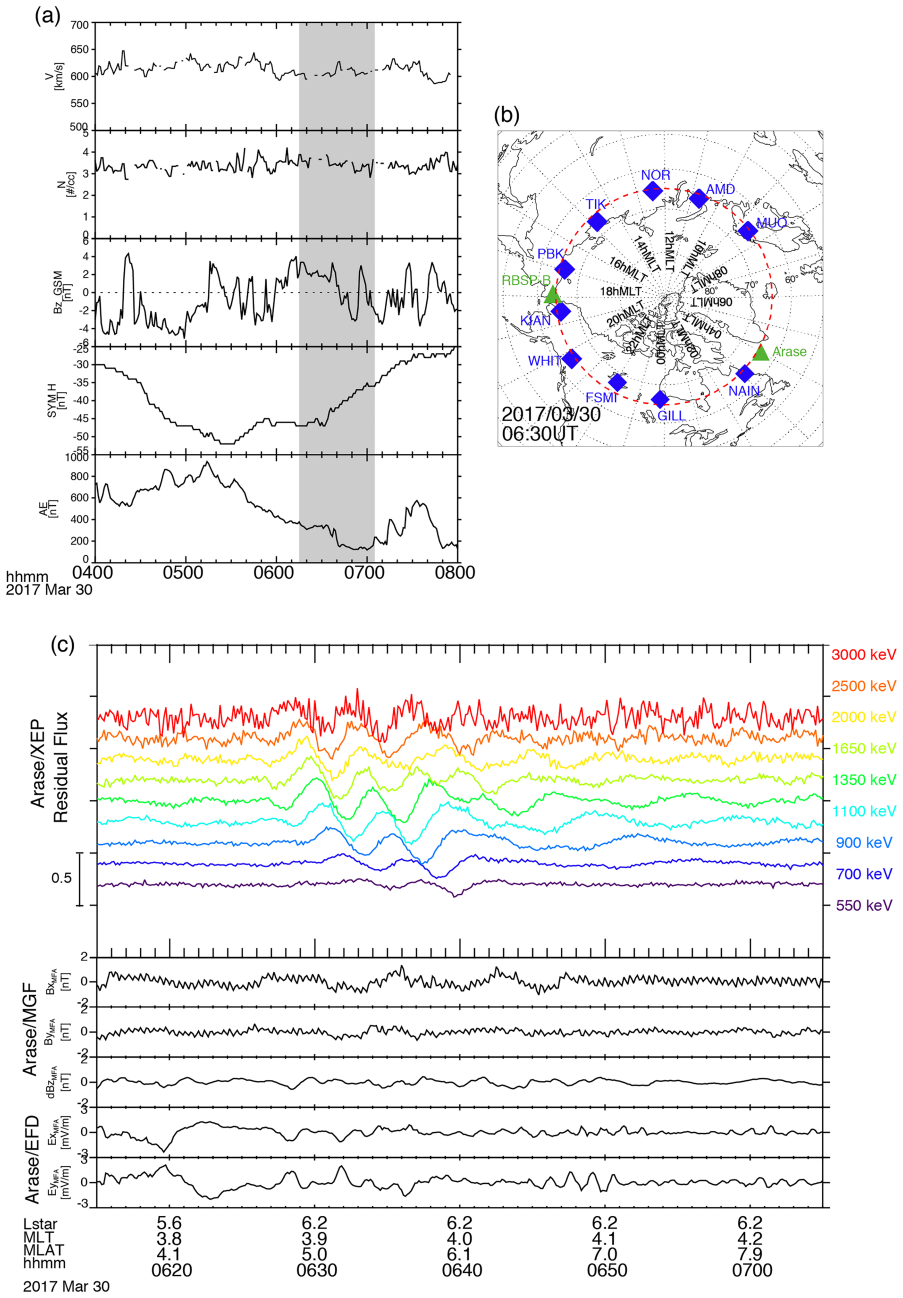

Figure 1. (a) Solar wind measurements and geomagnetic indices. (b) Locations of ground stations (blue diamond symbol) and footprint of Arase and Radiation Belt Storm Probe-B (green triangle symbol) estimated with the Tsyganenko 96 model field at 06:30UT on 30 March 2017 in Altitude-Adjusted Corrected GeoMagnetic coordinate (AACGM) and Magnetic Local Time (MLT). The red dash circle indicates 65º geomagnetic latitude. (c) The residual electron flux from XEP/Arase (top) and the magnetic field in the mean field-aligned coordinate system from MGF/Arase and EFD/Arase (bottom).

speed coronal hole streams (Miyoshi et al., 2013) were observed during this period, and the highest solar wind speed was ~600 km/s. The shaded region in Figure 1a corresponds to the time interval when Arase and RBSP-B observed energetic electron modulations in the ULF frequency range in the outer radiation belt. Figure 1b represents the locations of the ground geomagnetic stations (blue diamonds) around 65° geomagnetic latitude (red dashed circle) and the ionospheric footprints of the Arase and RBSP-B

satellites (green triangles) in Altitude Adjusted Corrected Geomagnetic Coordinates (Baker and Wing, 1989) at 06:30UT. The satellite footprints were estimated by mapping along magnetic field lines of the Tsyganenko T96 model (Tsyganeko,1995) driven by the observed IMF and solar wind pressure shown in Figure 1a. Arase was located slightly to the east of Nain (NAIN), and RBSP-B was located between Pevek (PBK) and Kiana (KIAN).

Figure 1c shows the residual electron fluxes from XEP/Arase for 550–2,140 keV. The residual flux at time t is defined as $(J(t) - J_0)/J_0$, where $J(t)$ is the spin-averaged electron flux observed in each energy channel of XEP and J_0 is the running average of $J(t)$ with a time window of 600 s centered around time t. Energetic electron fluxes were periodically modulated with periods of ~170-250 s, i.e., in the Pc5 frequency range and had an isolated spectral enhancement at 4-6 mHz (see Text S1 in the Supporting Information). Clear energy dispersion signatures in the electron fluxes indicate that higher energy electrons had arrived earlier. The bottom three and two panels in Figure 1c show the ambient magnetic and electric field variations measured by MGF/Arase and EFD/Arase, respectively. The MGF and EFD data are shown in the mean field-aligned (MFA) coordinate system; i.e., the $\mathbf{e_z}$ is in the direction of the 600-sec averaged magnetic field (the compressional component). The $\mathbf{e_x}$ and $\mathbf{e_y}$ components are directed radially outward (the radial component) and eastward (the azimuthal component), respectively, in the plane perpendicular to the averaged magnetic field. No ULF wave activity was observed by either the MGF or the EFD during this period, indicating that the electron flux modulations occurred at a different MLT.

The residual electron fluxes observed by XEP/Arase show clear energy dispersions, and we estimated the source region using a time-of-flight analysis. Considering the azimuthally localized drift resonance region, the phase lags of the electron fluxes near the resonant energies in the drift resonance region are shorter than those observed at different local times (Hao et al., 2017). Although we do not know the exact phase lags of the electron fluxes, now we assume that electrons forming the flux modulations are accelerated simultaneously at the source region and magnetic drifted into the region of the satellite position. As indicated in Figure 2a, the times of the electron flux peaks shown with the vertical lines are 06:33:03 UT (Δt = 215 s) for 550-keV electrons and 06:29:28 UT (Δt = 0 s) for 2.0-MeV electrons, where Δt is the elapsed time from 06:29:28 UT. We calculated the electron trajectories for 550 keV and 2.0 MeV using GEMSIS-RB, which is a relativistic electron tracing code (Saito et al., 2010). As an ambient magnetic field model, we used the Tsyganenko 04 model (Tsyganenko & Sitnov, 2005) with the observed solar wind data in Figure 1(a). The magnitude of the magnetic field observed by Arase is 1.02 times larger than that of the Tsyganenko 04 model field, indicating that the observed magnetic field is almost comparable to the model. We calculated backward-trajectory of many electrons at various energies and 90° pitch angle from the Arase satellite position. As shown in Figure 2b, the 550-keV and 2.0-MeV electrons were backtraced from the initial MLT at Δt = 210 s and Δt = 0 s, respectively. The trajectories of the energetic electrons cross at ~18 MLT and Δt = ~−90 s, indicating a modulation region for electrons with energies of 550 keV and 2. MeV. We applied this method to three peaks and three valleys and the pair of each energy channel with energies ranging from 550 keV to 3.0 MeV. Figure 2c shows the MLT distributions of the estimated source regions. Most of these regions lie in the range 15–18 MLT, with the maximum occurrence at 15–16 MLT. Applying this TOF analysis for the energetic electrons with the 90° pitch angles in the magnetic equator from the Arase MLT, the error of the estimated MLT is less than 0.72 hr. The pitch angle difference does not affect the MLT distribution in Figure 2c.

If the electron flux modulations occur on the duskside as the preceding calculations suggest, the ULF waves responsible for the flux modulations should be observed in this region. To investigate the ULF activities on the duskside, we analyzed the ground magnetic field data using the Time History of Event and Macroscale Interactions During Substorm network of ground magnetometers (Angelopoulos, 2008). Figure 3 presents the Y component of the geomagnetic field data on the ground for ~08 to ~03 MLT at nearly the same geomagnetic latitude of 64–68° MLat. Pc5 pulsations with isolated spectral enhancements at 4-6 mHz appeared at Tiksi (TIK), Pevek (PBK), and Kiana (KIAN) located in the postnoon to dusk sector (14–18MLT), while there were no ULF waves at Gilliam (GILL), Whitehorse (WHIT), Fort Simpson (FSIM), and Nain (NAIN) in the night sector at 24–04 MLT (See Text S2). Such Pc5 pulsations with isolated spectral enhancements are also observed in the X components by PBK, and KIAN and WHIT (see Text S3). The regions in which Pc5 pulsations were observed corresponding to the estimated source regions of the energetic electron flux modulations observed by Arase. We estimated the azimuthal wave numbers of the Pc5 pulsations on the ground from the

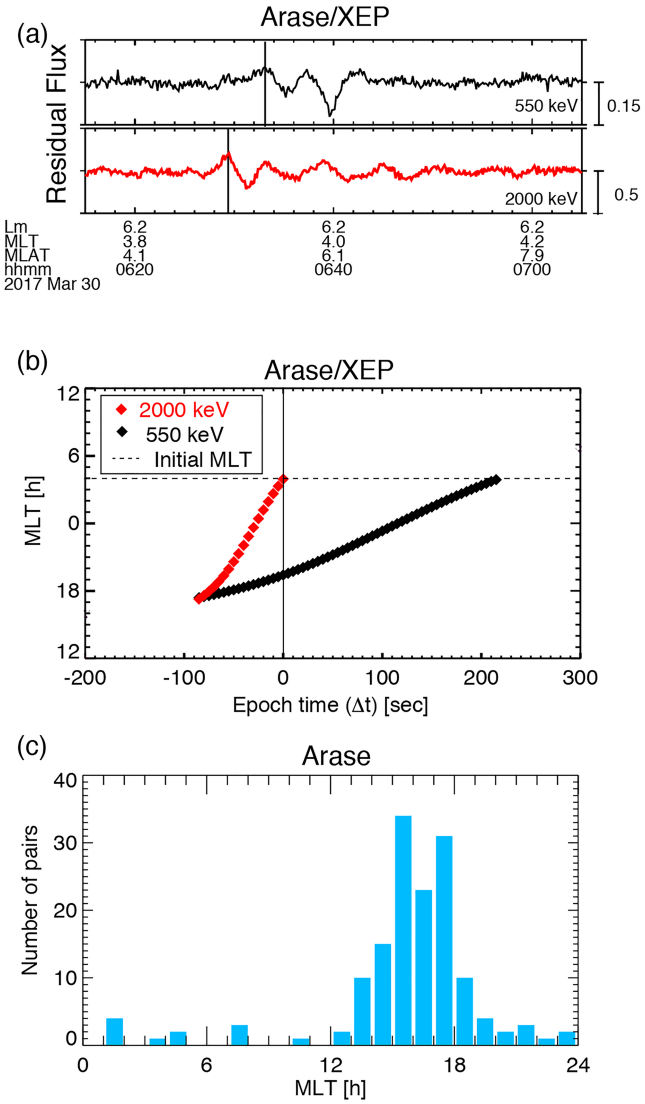

Figure 2. (a, b) An example of an estimation of the source region of the relativistic flux modulations from XEP/Arase. (a) Residual fluxes at 550 keV and 2.0 MeV. (b) The energetic electron trajectories at 550 keV and 2.0 MeV via backtracking in the Tsyganenko 04 model. (c) Histogram of the estimated source regions using the backtracking method.

phase differences between PBK and KIAN (TIK and PBK). A fast Fourier transform analysis was applied to the magnetic field data at PBK and KIAN (TIK and PBK), from which the 20-min running averages were subtracted, with a 33-min time window from 6:20 to 6:53 UT. The cross-phase, $\Delta\theta$, of the Y component at KIAN (PBK) relative to that at PBK (TIK) was −114° (−98°) at 5 mHz. Given the longitudinal difference, $\Delta\varphi$, of approximately 28° (33°) between the two stations, the azimuthal wave number is estimated to be ~4 (~3) with an eastward propagation based on the equation $m = \Delta\theta/\Delta\varphi$. Pc5 pulsations also occurred at Muono (MUO), Amderma (AMD), and Norilsk (NOR), located at 8–13MLT. With the phase difference of ULF waves at MUO and AMD, we estimate an azimuthal wave number of ~6 with a westward propagation in the dawn sector.

During this time period, RBSP-B was on the duskside at ~18 MLT, and the ionospheric footprint was close to KIAN. Figure 4a represents the residual flux of the energetic electrons with energies ranging from 600 keV to 2.6 MeV from MagEIS and the magnetic field from EMFISIS. The frequency of electron flux modulations and magnetic field perturbations are almost same as those of the electron modulations observed by XEP and Pc5 pulsations on the duskside ground stations (see Text S4). The time lags of the peaks from

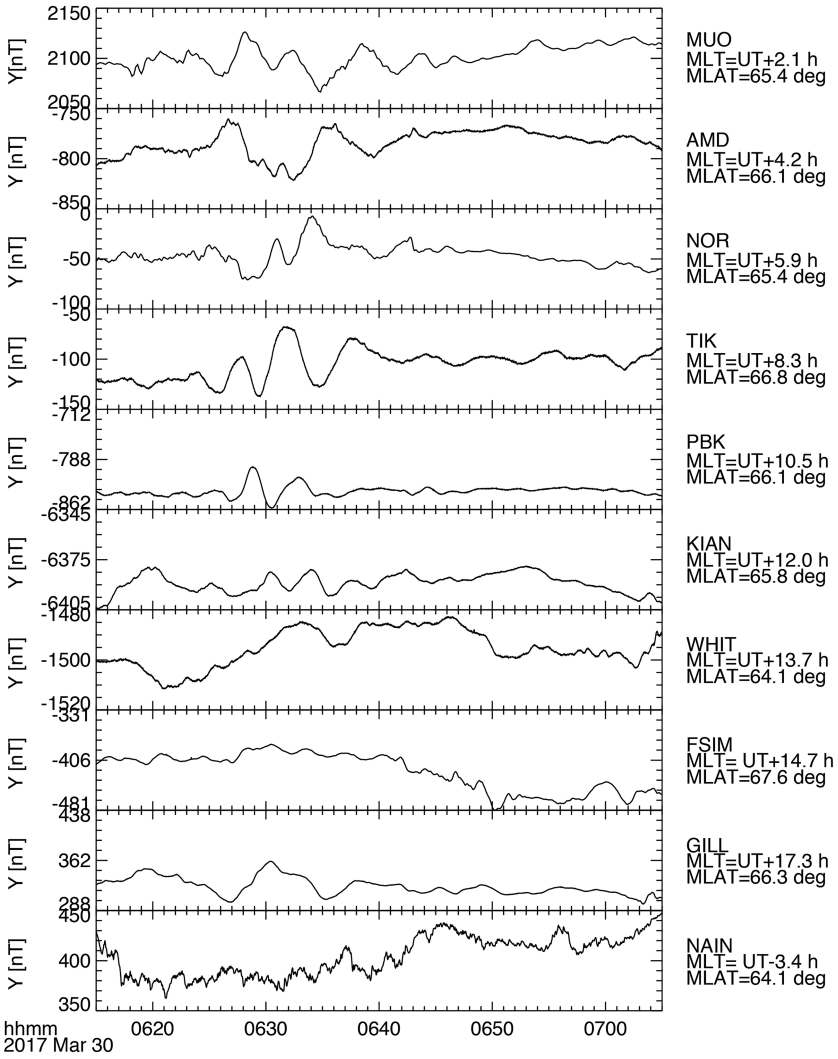

Figure 3. The *Y* component of the geomagnetic field data at Muono, Amderma, Norilsk, Tiksi, Pevek, Kiana, Whitehorse, Fort Simpson, Gilliam, and Nain.

lower energy to higher energy are much smaller than those of Arase, suggesting that RBSP-B was close to the modulation region. The compressional component of the magnetic field at RBSP-B oscillates at the Pc5 period of ~250 s with an amplitude of ~1 nT. To identify the dominant frequency of the residual flux and the cross phase of the residual flux relative to the Pc5 pulsations in the compressional component, we applied an FFT analysis with an 8-min time window from 6:27 to 6:35 UT after 10-min running averages of the magnetic field were subtracted from the original geomagnetic field data. Figures 4b and 4c represent the power spectra of the residual flux at 5–6 mHz and the cross phase of the residual fluxes relative to the Pc5 pulsations at 5–6 mHz as a function of energy, respectively. Note that the residual flux modulations have a maximum amplitude at 1 MeV, at which the phase at 5.5 mHz becomes 90° relative to magnetic field data. These features are consistent with the drift-resonance theory of Southwood and Kivelson (1981, 1982). We estimate the m number for the drift resonance condition described as equation (1). The azimuthal drift frequency of a 1.0-MeV electron with a 90° pitch angle at the magnetic equator is ~1.3 mHz at L ~ 6 in a dipole field (Walt, 1994). Using this drift frequency and the observed ULF wave frequency (5.5 mHz), the m number is estimated as ~4.2, which is consistent with ground observations. This consistent result provides further support for the interpretation based on drift resonance.

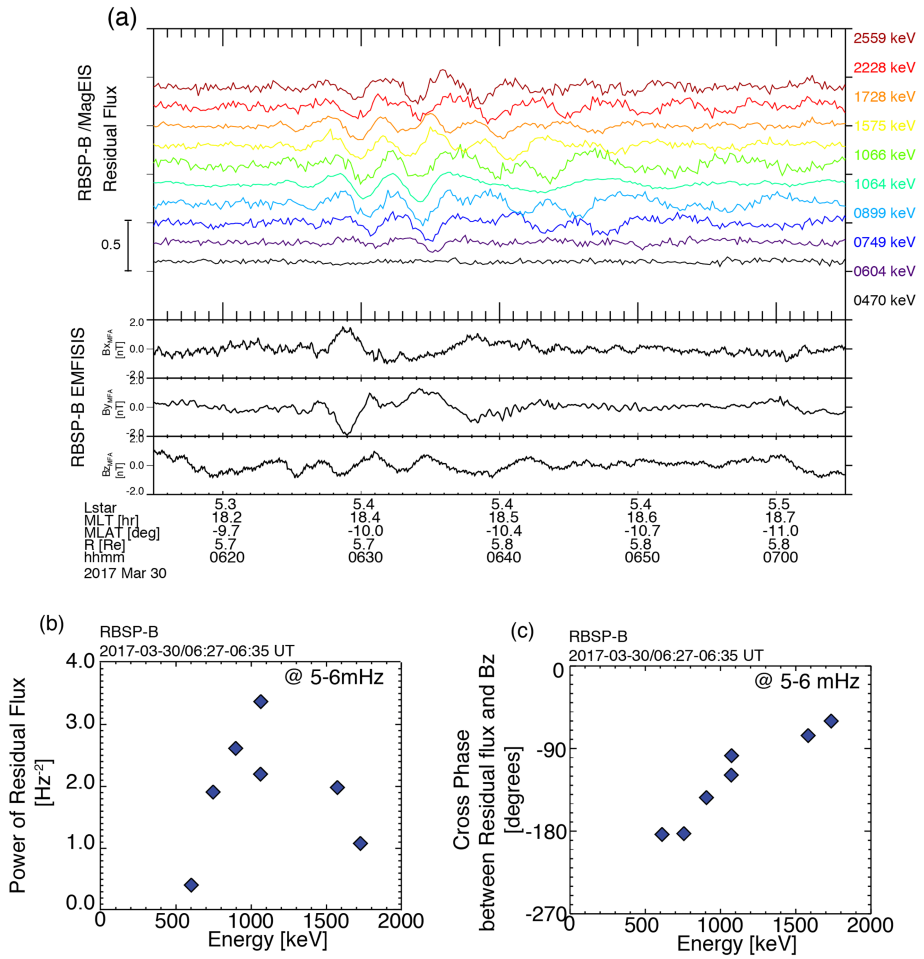

Figure 4. (a) The residual electron flux from MagEIS-B (top) and the magnetic field in the mean field-aligned coordinate system from EMFISIS-B magnetometer (bottom). (b) Power of the residual flux from MagEIS at 5–6 mHz and (c) the phase difference of the residual flux modulations from MagEIS relative to the magnetic field modulations in the compressional component from EMFISIS at 5–6 mHz as a function of energy.

4. Summary and Discussion

The observational results are summarized as follows: (a) energetic electron flux modulations at the Pc5 frequency with an energy dispersion signature from 550 keV to 3.0 MeV were observed in the morning local time sector by the Arase satellite, and corresponding ULF waves were not observed in the electric and magnetic field; (b) RBSP-B observed energetic electron modulations with nearly the same frequency as the Pc5 pulsations in the ambient magnetic field. The drift resonance occurred during the period as indicated by the energy dependence of the power and phase of the residual flux relative to the magnetic field at a frequency of 5.5 mHz; (c) Multipoint ground magnetometers observed eastward-propagating Pc5 pulsations with a small m number of ~4 in the afternoon-dusk sector of 14–18 MLT, which is consistent with the source region based on the relativistic electron observations.

From these observations, we suggested the following processes as the origin of the periodic flux oscillations observed by Arase. First, the energetic electrons drifting eastward around the Earth go through the afternoon-dusk sector, in which Pc5 pulsations are propagating eastward. In this region, the Pc5 pulsations modulate the energetic electron flux near the energy of 1 MeV via drift resonance interaction. After modulation in the afternoon-dusk sector, the energetic electrons further drift eastward in the dusk-night-morning sector without corresponding ULF waves. These oscillations have energy dispersion signatures because the drift velocity of the electrons is dependent on their energy.

The drift resonance interaction observed on the duskside is likely due to the fundamental poloidal mode Pc5 pulsations. Assuming that the proton number density is comparable to the local electron number density of ~50 cm^{-3}, which was obtained from the RBSP-B between 6:20 and 6:30 UT at $L \sim 5.5$, we estimate the fundamental poloidal eigenfrequency (f_0) of a flux tube using the numerical result of Cummings et al. (1969), and Orr and Matthew (1971) obtained f_0 ~ 3–4 mHz, which is consistent with our observation. Pulsations in the *Y* component on the ground at high latitudes correspond to a poloidal mode wave in the magnetosphere, considering that the magnetic polarization of Alfven waves is rotated by roughly 90° when they pass through the conducting ionosphere and the magnetic field is nearly vertical to the ionosphere (Hughes & Southwood, 1976).

The poloidal mode waves in the magnetosphere had oscillations in the compressional and radial components of the magnetic field, in addition to the azimuthal component of the electric field. At the magnetic equator, the electric field perturbations in the azimuthal component are much easier to identify than the magnetic field perturbation in the radial component because fundamental Pc5 pulsations in the magnetic and electric fields have a node and an antinode, respectively, at the magnetic equator. However, we could not obtain the azimuthal component for this event because the ambient magnetic field direction was almost parallel to the spin plane of the RBSP-B. Instead of the azimuthal component of the electric field, we investigated the energy dependence of the cross phase between electron flux modulations and the Pc5 pulsations in the compressional component of the magnetic field.

So far, we estimated the source regions located at 15–18 MLT, by assuming that electrons that form the flux modulations were accelerated simultaneously at the source region. However, as shown from the RBSP-B observations, flux modulations of energetic electrons in the drift resonance region have slight lag times across the resonance energy. In fact, the phase shift of energetic electron modulations across the frequency of the power maximum provides an evidence that the drift resonance interaction took place at or near the RBSP-B position on the duskside (Claudepierre et al., 2013). If we consider this possibility, the actual drift resonance region is located eastward of the estimated source region. Applying the time-of-flight technique with this assumption, the lag times estimated based on XEP observations were almost consistent with those actually observed by the RBSP-B (not shown). This estimation indicates that the flux modulations of the XEP just drifted from the RBSP-B location to the Arase location.

Periodic energetic electron modulations without ULF waves are frequently observed. Using the RBSP-B satellite, Hao et al. (2017) showed that energetic electrons with energy near 450 keV had periodic dispersion signatures in the pitch angle spectra when RBSP-B was located on the morning side after the arrival of an interplanetary shock, and corresponding ULF waves were not observed in the magnetic and electric fields. Applying a time-of-flight technique similar to that presented in this paper and numerical calculations to the energetic electrons, they also suggested that the ULF waves localized on the duskside accelerate energetic electrons in that region. After three cycles of electron flux modulations appear, the flux modulations of the energetic electrons observed by both RBSP-B and Arase exhibit the signature of drift echoes, for which the period of modulation at lower energies becomes longer. These features are also consistent with the drift resonance between azimuthally localized damping ULF waves and energetic electrons (Hao et al., 2017; Zhou et al., 2016; Zong et al., 2017). Due to the lack of observational data for the noon-dusk side, Hao et al. (2017) indirectly estimated the *m* number of Pc5 pulsations on the duskside from the periods of the flux modulations. The *m* number estimated by Hao et al. (2017) was ~6. Using the data set of the magnetic field and the energetic electron flux from the RBSP-B and the magnetic field data on the ground, we confirm that the ULF with an asymmetric low *m* number of ~4 interacts with the energetic electrons with an energy of approximately 1 MeV.

This study suggests that periodic energetic electron modulations without local ULF activity are the result of a "remote" drift-resonance interaction with the energetic electrons and the ULF waves. In general, the radial diffusion coefficients are derived based on measurements of the power spectral densities observed by satellites or ground stations (e.g., Ozeke et al., 2012), assuming that ULF waves with small *m* numbers are globally excited. However, our results indicate that the azimuthal distributions of ULF waves as well as the latitudinal distributions of these waves can be limited. It is expected that the radial diffusion coefficients will be modified if we consider a realistic azimuthal distribution of ULF waves, which could contribute to some improvements in the radiation belt modeling.

From the observational features that the Pc5 pulsations propagate eastward in the noon-dusk sector and have a small *m* number, we consider that the Pc5 pulsations observed in this study are likely driven by external sources: solar wind dynamic pressure perturbation (Viall et al., 2009) or Kelvin-Helmholtz (K-H) waves generated at the magnetopause (Agapitov et al., 2009; Rae et al., 2005). Attenuation of Pc5 pulsations with small *m* numbers is caused by the spatial structure of the source region. Numerical simulation studies on ULF waves driven by solar wind dynamic pressure variations and K-H instabilities show that ULF waves appear dominantly on the dayside (Claudepierre et al., 2010) and flank side (Claudepierre et al., 2008), respectively. The periodic modulations with the same period as the Pc5 pulsations do not appear in the solar wind number density although the solar wind speed is quite high. These solar wind conditions might support K-H instabilities rather than dynamic pressure perturbations as the possible generation mechanism of these Pc5 pulsations. In the realistic magnetosphere, externally driven ULF waves might have an azimuthally limited structure even though their wave numbers are small.

Acknowledgments
Solar wind data time-shifted to the bow shock nose were obtained from the OMNI database, which were provided by the Space Physics Data Facility of Goddard Space Flight Center. SYM-H and *AE* indices were provided by the World Data Center for Geomagnetism, Kyoto, Kyoto University. The distribution of SYM-H and *AE* indices are partly supported by the IUGONET (Inter-university Upper atmosphere Global Observation NETwork) project (http://www.iugonet.org/). M. T. is supported by the JSPS grant (19K03948). Y. M. is supported by the JSPS grant (15H05815, 15H05747, and 16H06286). I. S. is supported by the JSPS grant (17H06140). Sience data of the ERG (Arase) satellite were obtained from the ERG Science Center (ERG Science Center) operated by ISAS/JAXA and ISEE/Nagoya University (https://ergsc.isee.nagoya-u.ac.jp/index.shtml.en), the works of M. T., T. H., and Y. M. were partly done at ERG-SC. Work at The Aerospace Corporations was supported by RBSP-ECT funding provided by JHU/APL contract 967399 under NASA's Prime contract NAS5-01072. The present study analyzed the MGF, the PWE/EFD, and the XEP data of v01.01, ver02.01, and ver00.00, respectively. The XEP data processing was partly supported by the SEES/JAXA. Geomagnetic field data from Tiksi and Pevek were provided by Arctic and Antarctic Research Institute. Geomagnetic field data from Kiana and Gillam are provided by the University of California, Los Angeles, and the University of Albata, respectively. *The authors thank M. J. Engebretson and the rest of the MACCS team for* Nain *data. MACCS is operated by Augsburg University and* funded by U.S. National Science Foundation grant AGS-1651263. The ground magnetometer of Norilsk was provided by A. Pashinin and N. Nishitani. These geomagnetic field data were downloaded with the SPEDAS software (http://spedas.org). This study was supported by JSPS Bilateral Open Partnership Joint Research Projects (1007752).

References

Agapitov, O., Glassmeier, K. H., Plaschke, F., Auster, H. U., Constantinescu, D., Angelopoulos, V., et al. (2009). Surface waves and field line resonances: A THEMIS case study. *Journal of Geophysical Research*, *114*(A1), A00C27. https://doi.org/10.1029/2008JA013553

Angelopoulos, V. (2008). The THEMIS mission. *Space Science Reviews*, *141*, 5–34. https://doi.org/10.1007/s11214-008-9336-1

Baker, K. B., & Wing, S. (1989). A new magnetic coordinate system for conjugate studies at high latitudes. *Journal of Geophysical Research*, *94*(A7), 9139. https://doi.org/10.1029/ja094ia07p09139

Blake, J., Carranza, P. A., Claudepierre, S. G., Clemmons, J. H., Crain, W. R., Dotan, Y., et al. (2013). The Magnetic Electron Ion Spectrometer (MAGEIS) instruments aboard the Radiation Belt Storm Probes (RBSP) spacecraft. *Space Science Reviews*, *179*(1–4), 383–421. https://doi.org/10.1007/s11214-013-9991-8

Claudepierre, S. G., Elkington, S. R., & Wiltberger, M. (2008). Solar wind driving of magnetospheric ULF waves: Pulsations driven by velocity shear at the magnetopause. *Journal of Geophysical Research*, *113*, A05218. https://doi.org/10.1029/2007JA012890

Claudepierre, S. G., Hudson, M. K., Lotko, W., Lyon, J. G., & Denton, R. E. (2010). Solar wind driving of magnetospheric ULF waves: Field line resonances driven by dynamic pressure fluctuations. *Journal of Geophysical Research*, *115*, A11202. https://doi.org/10.1002/2015JA022048

Claudepierre, S. G., Mann, I. R., Takahashi, K., Fennell, J. F., Hudson, M. K., Blake, J. B., et al. (2013). Van Allen Probes observation of localized drift resonance between poloidal mode ultra-low frequency waves and 60 keV electrons. *Geophysical Research Letters*, *40*, 4491–4497. https://doi.org/10.1002/grl.50901

Cummings, W. D., O'Sullivan, R. J., & Coleman, P. J. Jr. (1969). Standing Alfvén waves in the magnetosphere. *Journal of Geophysical Research*, *74*(3), 778–793. https://doi.org/10.1029/JA074i003p00778

Elkington, S. R., Hudson, M. K., & Chan, A. A. (1999). Acceleration of relativistic electrons via drift resonant interaction with toroidal-mode Pc-5 ULF oscillations. *Geophysical Research Letters*, *26*(21), 3273. https://doi.org/10.1029/1999GL003659

Hao, Y. X., Zong, Q.-G., Zhou, X.-Z., Rankin, R., Chen, X. R., Liu, Y., et al. (2017). Relativistic electron dynamics produced by azimuthally localized poloidal mode ULF waves: Boomerang-shaped pitch angle evolutions. *Geophysical Research Letters*, *44*, 7618–7627. https://doi.org/10.1002/2017GL074006

Higashio, N., Takashima, T., Shinohara, I., & Matsumoto, H. (2018). The extremely high-energy electron experiment (XEP) onboard the Arase (ERG) satellite. *Earth, Planets and Space*. https://doi.org/10.1186/s40623-018-0901-x

Hughes, W. J., & Southwood, D. J. (1976). The screening of micropulsation signals by the atmosphere and ionosphere. *Journal of Geophysical Research*, *81*, 3234–3240. https://doi.org/10.1029/JA81i019p03234

Kasaba, Y., Ishisaka, K., Kasahara, Y., Imachi, T., Yagitani, S., Kojima, H., et al. (2017). Wire Probe Antenna (WPT) and Electric Field Detector (EFD) of Plasma Wave Experiment (PWE) aboard the Arase satellite: Specifications and initial evaluation results. *Earth, Planets and Space*, *69*(1), 174. https://doi.org/10.1186/s40623-017-0760-x.

Kasahara, Y., Kasaba, Y., Kojima, H., Yagitani, S., Ishisaka, K., Kumamoto, A., et al. (2018). The Plasma Wave Experiment (PWE) on board the Arase (ERG) satellite. *Earth, Planets and Space*, *70*(1). https://doi.org/10.1186/s40623-018-0842-4

Kletzing, C., Kurth, W. S., Acuna, M., MacDowall, R. J., Torbert, R. B., Averkamp, T., et al. (2013). The Electric and Magnetic Field Instrument Suite and Integrated Science (EMFISIS) on RBSP. *Space Science Reviews*, *179*, 127–181.

Mathie, R., & Mann, I. (2000). A correlation between extended intervals of ULF wave power and storm-time geosynchronous relativistic electron flux enhancements. *Geophysical Research Letters*, *27*(20), 3261–3264. https://doi.org/10.1029/2000GL003822

Matsuoka, A., Teramoto, M., Nomura, R., Nosé, M., Fujimoto, A., Tanaka, Y., et al. (2018). The ARASE (ERG) magnetic field investigation. *Earth, Planets and Space*, *70*(1). https://doi.org/10.1186/s40623-018-0800-1

Miyoshi, Y., Kataoka, R., Kasahara, Y., Kumamoto, A., Nagai, T., & Thomsen, M. F. (2013). High-speed solar wind with southward interplanetary magnetic field causes relativistic electron flux enhancement of the outer radiation belt via enhanced condition of whistler waves. *Geophysical Research Letters*, *40*, 4520–4525. https://doi.org/10.1002/grl.50916

Miyoshi, Y., Shinohara, I., Takashima, T., Asamura, K., Higashio, N., Mitani, T., et al. (2018). Geospace Exploration Project ERG. *Earth, Planets and Space*, *70*(1). https://doi.org/10.1186/s40623-018-0862-0

Orr, D., & Matthew, J. A. D. (1971). The variation of geomagnetic micropulsation periods with latitude and the plasmapause. *Planetary and Space Science*, *19*, 897–905. https://doi.org/10.1016/0032-0633(71)9041-3.

Ozeke, L. G., Mann, I. R., Murphy, K. R., Rae, I. J., & Milling, D. K. (2013). Analytic expressions for ULF wave radiation belt radial diffusion coefficients. *Journal of Geophysical Research: Space Physics*, *119*, 1587–1605. https://doi.org/10.1002/2013JA019204

Ozeke, L. G., Mann, I. R., Murphy, K. R., Rae, I. J., Milling, D. K., Elkington, R., et al. (2012). ULF wave derived radiation belt radial diffusion coefficients. *Journal of Geophysical Research*, *117*, A04222. https://doi.org/10.1029/2011JA017463

Rae, I. J., Donovan, E. F., Mann, I. R., Fenrich, F. R., Watt, C. E. J., Milling, D. K., et al. (2005). Evolution and characteristics of global Pc5 ULF waves during a high solar wind speed interval. *Journal of Geophysical Research*, *110*(A12), A12211. https://doi.org/10.1029/2005JA011007.

Saito, S., Miyoshi, Y., & Seki, K. (2010). A split in the outer radiation belt by magnetopause shadowing: Test particle simulations. *Journal of Geophysical Research*, *110*, A12211. https://doi.org/10.1029/2009JA014738

Shprits, Y. Y., Elkington, S. R., Meredith, N. P., & Subbotin, D. A. (2008). Review of modeling on losses and sources of relativistic electrons in the outer radiation belt I: Radial transport. *Journal of Atmospheric and Solar: Terrestrial Physics*, *70*, 1679–1693. https://doi.org/10.1016/j.jastp.2008.06.008

Southwood, D. J., Dungey, J. W., & Etherington, R. J. (1969). Bounce resonant interactions between pulsations and trapped particles. *Planetary and Space Science*, *17*, 349. https://doi.org/10.1016/0032-0633(69)90068-3

Southwood, D. J., & Kivelson, M. G. (1981). Charged particle behavior in low-frequency geomagnetic pulsations: 1. Transverse waves. *Journal of Geophysical Research*, *86*, 5643–5655. https://doi.org/10.1029/JA086iA07p05643

Southwood, D. J., & Kivelson, M. G. (1982). Charged particle behavior in low-frequency geomagnetic pulsations: 2. Graphical approach. *Journal of Geophysical Research*, *87*, 1707–1710. https://doi.org/10.1029/JA087iA03p01707

Tan, L. C., Fung, S. F., & Shao, X. (2004). Observation of magnetospheric relativistic electrons accelerated by Pc-5 ULF waves. *Geophysical Research Letters*, *31*, L14802. https://doi.org/10.1029/2004GL019459

Tan, L. C., Shao, X., Sharma, A. S., & Fung, S. F. (2011). Relativistic electron acceleration by compressional-mode ULF waves: Evidence from correlated Cluster, Los Alamos National Laboratory spacecraft, and ground-based magnetometer measurements. *Journal of Geophysical Research*, *116*, A07226. https://doi.org/10.1029/2010JA016226

Tsyganenko, N. A., & Sitnov, M. I. (2005). Modeling the dynamics of the inner magnetosphere during strong geomagnetic storms. *Journal of Geophysical Research*, *110*, A03208. https://doi.org/10.1029/2004JA010798

Viall, N. M., Kepko, L., & Spence, H. E. (2009). Relative occurrence rates and connection of discrete frequency oscillations in the solar wind density and dayside magnetosphere. *Journal of Geophysical Research*, *114*, A01201. https://doi.org/10.1029/2008JA013334.

Walt, M. (1994). *Introduction to geomagnetically trapped radiation*. New York: Cambridge Univ. Press.

Zhou, X. -Z., Wang, Z.-H., Zong, Q.-G., Rankin, R., Kivelson, M. G., Chen, X.-R., et al. (2016). Charged particle behavior in the growth and damping stages of ultralow frequency waves: Theory and Van Allen Probes observations. *Journal of Geophysical Research: Space Physics*, *121*, 3254–3263. https://doi.org/10.1002/2016JA022447

Zong, Q., Rankin, R., & Zhou, X. (2017). The interaction of ultra-low-frequency Pc3-5 waves with charged particles in Earth's magnetosphere. *Reviews of Modern Plasma Physics*, *1*, 10. https://doi.org/10.1007/s41614-017-011-4

Zong, Q.-G., Zhou, X.-Z., Wang, Y. F., Li, X., Song, P., Baker, D. N., et al. (2009). Energetic electron response to ULF waves induced by interplanetary shocks in the outer radiation belt. *Journal of Geophysical Research*, *114*, A10204. https://doi.org/10.1029/2009JA014393